

title

X. Y. Jimmy^{a,*}, P. F. Mendez^a

^aDepartment of Chemical and Materials Engineering, University of Alberta, Edmonton, Alberta, T6G 2V4, Canada

Abstract

Abstract goes here

Keywords: keyword1, keyword2, keyword3, keyword4

1. Introduction

introsection from Mathes *et al.*, [1, 2], at 700 °C, and 300μm

$$\begin{aligned} P &= 7 \times C + 5 \times Si - 3 \times Mn + 8 \times Nb \\ &: C, Si, Mn, Nb(\text{wt\%}) \end{aligned} \tag{1}$$

[Eq. 1](#) in [3].

2. Experimental

2.1. Materials

Experimental section. M₂₃C₆

Table 1: Composition of the ex-service 2032-Nb stainless steel alloy

	Composition (wt%)							
	Cr	Ni	Mn	Si	C	Nb	N	W,Mo,Ti,Zr
2032Nb	20.6	32.7	0.96	1.00	0.086	1.13	0.051	< 0.05

2.2. Chemical analysis

[Table 1](#)

*Corresponding author. Tel: +1-780-XXX-XXXX
Email addresses: jimmy@ualberta.ca (X. Y. Jimmy), pmendez@ualberta.ca (P. F. Mendez)

3. Results

3.1. Model

The shear stress varies little within a thin shear layer, and will be assumed to have a constant value τ_c in that region. Also, considering that the shear rate and velocity gradient are essentially the same magnitude ($\dot{\gamma} = -dv/dx$) we can restate as

$$q(x) = -\eta_s \tau_c \frac{dv}{dx} \quad (2)$$

with boundary condition $v = \omega a$ at $x = 0$. The two terms of Eq. 2 can be normalized by an estimation of their maximum values obtaining

$$q_c q^* = -\frac{3}{2} \eta_s \tau_c \frac{\omega a}{\delta} \left(\frac{dv}{dx} \right)^* \quad (3)$$

where the magnitudes with an asterisk have been normalized by an estimation of their maximum value. The factor of 3/2 present in the normalization of the derivative relates to the evolution of velocity within the shear layer illustrated in. Replacing the normalized functions by +1 or -1, Eq. 3 turns into the following algebraic equation based on characteristic values:

$$\hat{q}_c = \frac{3}{2} \eta_s \hat{\tau}_c \frac{\omega a}{\hat{\delta}} \quad (4)$$

Eq. 4 introduces one new unknown characteristic value: $\hat{\tau}$.

Near the incipient melting temperature, the Arrhenius component can be linearized as

$$\exp \left(-\frac{Q}{RT_s} \right) \approx \begin{cases} 0 & \text{if } T \leq T_0 \\ \frac{\hat{T}_s - T_0}{T_m - T_0} \exp \left(-\frac{Q}{RT_m} \right) & \text{if } T > T_0 \end{cases} \quad (5)$$

where T_m is the temperature of incipient melting of the material, whether its solidus temperature or some critical low melting temperature eutectic.

3.2. Chemistries

The results in Table 2

Table 3 includes the area fraction, and precipitate diameter for each phase characterized in AES, and SEM. For every phase except Z-phase, Area fractions were obtained by EPMA elemental mapping on the center of each sample. The resolution of the elemental maps was $1\mu\text{m}/\text{pixel}$, at a dwell time of 20ms, where the area fractions were calculated from a total area of 531mm^2 .

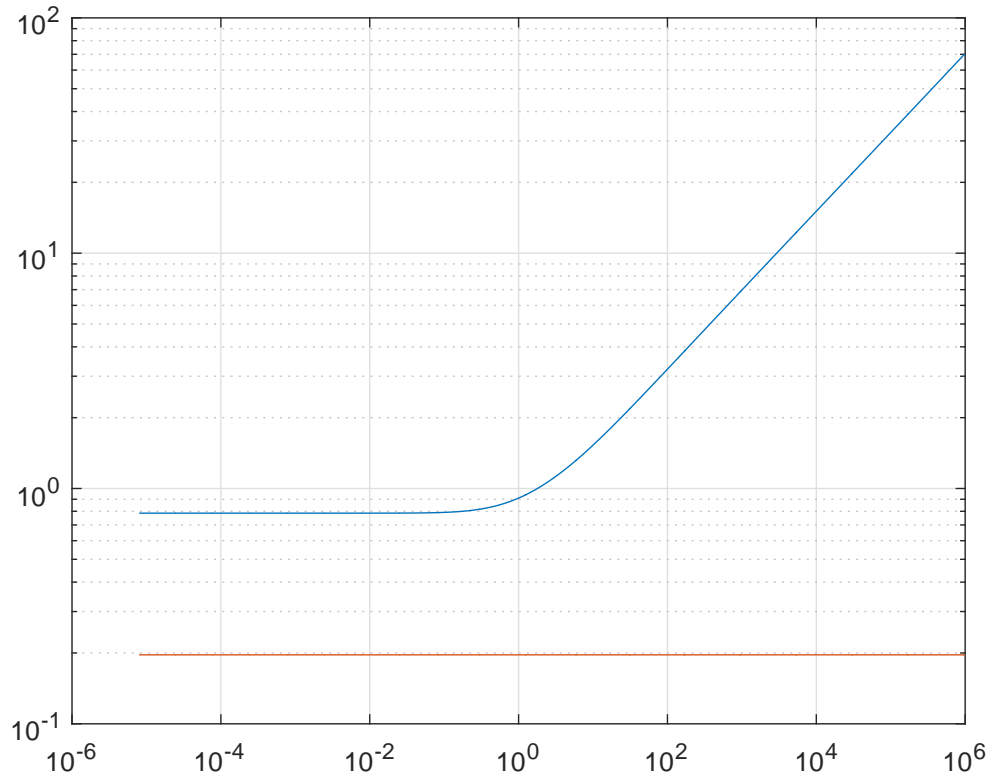


Fig. 1: Ratio of maximum temperature in the base plate f_T . The four hypotheses are fulfilled and the ratio remains relatively constant and close to unity.

Table 2: Phase composition in wt% (brackets in at%) on the microstructure of a fully aged centrifugally cast 20Cr-32Ni-1Nb stainless steel sample. Compositional data was gathered using AES quantitative Analysis.

Phase	Fe	Ni	Cr	Composition, wt% (at%)				Number of Points
				Si	Nb	C	N	
Fully Aged								
γ -Fe (boundary)	bal	36.7 ± 1.6 (32.3 ± 2.0)	17.50 ± 3.8 (17.3 ± 3.2)	-	-	2.43 ± 1.4 (10.2 ± 5.6)	-	4
Z-Phase	bal	1.4 ± 1.6 (1.2 ± 1.4)	31.1 ± 1.2 (29.2 ± 0.7)	0.2 ± 0.6 (0.4 ± 1.0)	55.4 ± 2.0 (29.1 ± 1.7)	1.4 ± 0.3 (5.6 ± 1.0)	9.7 ± 0.8 (33.9 ± 2.0)	14
$M_{23}C_6$	bal	3.3 ± 0.6 (2.5 ± 0.5)	82.7 ± 0.7 (70.9 ± 1.7)	-	-	5.3 ± 0.6 (19.6 ± 2.0)	-	12
G-Phase	bal	52.0 ± 3.4 (48.6 ± 2.9)	0.3 ± 0.6 (0.3 ± 0.6)	11.6 ± 1.5 (22.5 ± 2.5)	33.6 ± 4.3 (20.0 ± 3.0)	1.1 ± 0.2 (5.2 ± 0.9)	0.7 ± 0.6 (2.8 ± 2.4)	14
$Nb(C,N)$	bal	7.3 ± 4.6 (5.1 ± 3.0)	3.1 ± 4.0 (2.6 ± 3.5)	1.0 ± 0.4 (1.1 ± 0.3)	69.2 ± 5.8 (31.1 ± 3.4)	12.2 ± 1.7 (42.2 ± 4.0)	5.5 ± 0.7 (16.4 ± 2.0)	14
Annealed								
$Nb(C,N)$	bal	4.8 ± 2.1 (4.1 ± 2.5)	1.9 ± 1.7 (1.8 ± 1.7)	1.1 ± 1.2 (1.9 ± 2.1)	74.2 ± 5.8 (39.2 ± 3.0)	8.9 ± 0.7 (36.5 ± 2.4)	3.3 ± 0.4 (11.4 ± 1.4)	25

Table 3: Particle diameter, and phase fraction (vol%) of a fully aged, and solution annealed 2032Nb microstructure.

Phase	Centrifugally Cast		
	particle Diameter (μm)	Number of Points	Phase Fraction (vol%)
Fully Aged			
Nb(C,N)	1.73 \pm 1.17	14	0.03 \pm 0.01
M ₂₃ C ₆	2.86 \pm 1.52	85	0.97 \pm 0.32
G-phase (interdendritic)	4.02 \pm 2.00	68	2.43 \pm 0.48
G-phase (intradendritic)	1.33 \pm 0.30	108	0.92 \pm 0.12
Z-phase	1.50 \pm 0.83	49	0.29 \pm 0.16
Solution Annealed			
Nb(C,N)	0.78 \pm 0.23	129	3.40 \pm 0.10

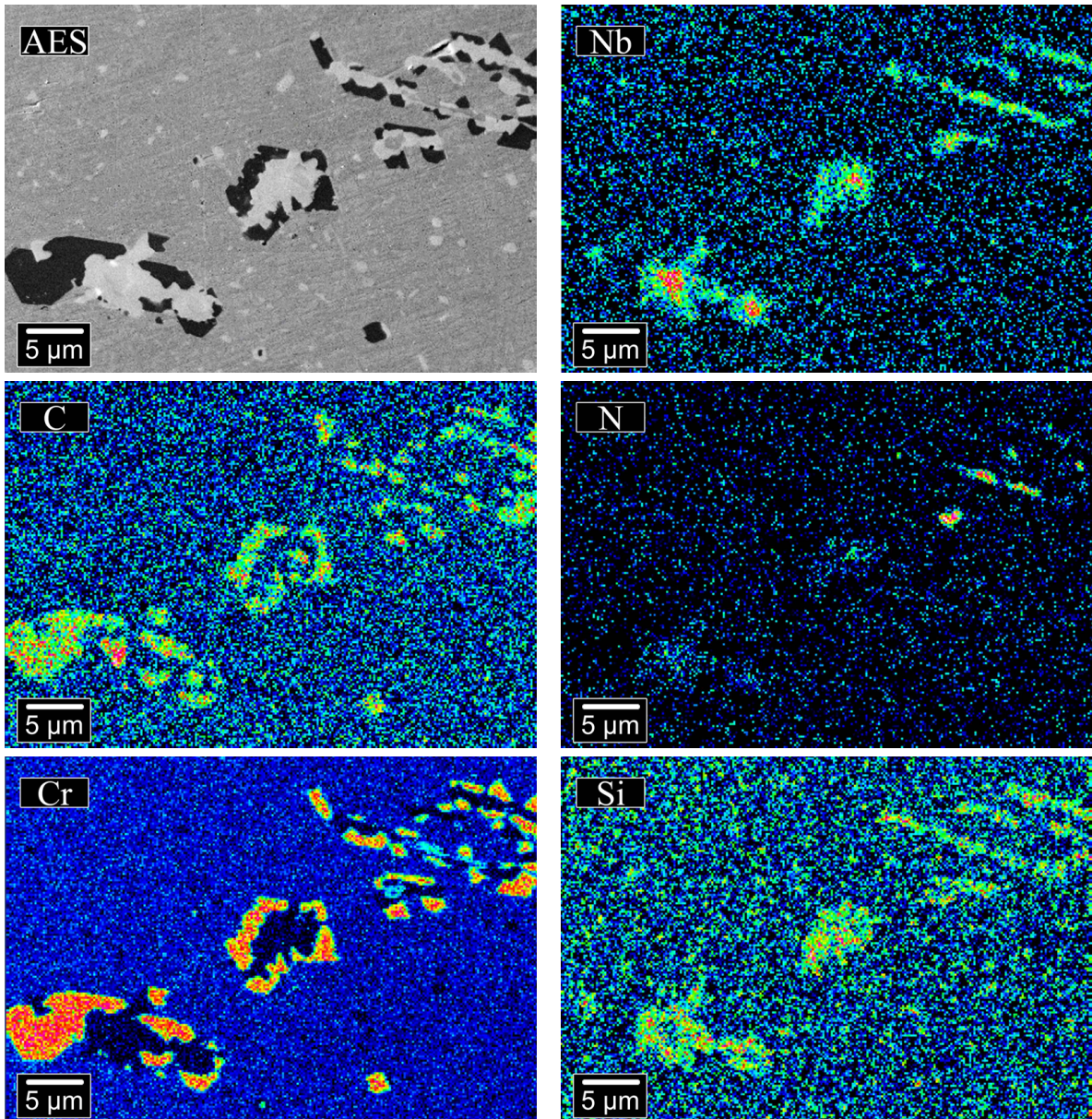


Fig. 2: Element maps from Auger Electron Spectroscopy of an interdendritic region of a fully aged 2032Nb Stainless steel pipe.

3.3. Phase Mapping

3.4. ThermoCalc & Compositional Factorial Design

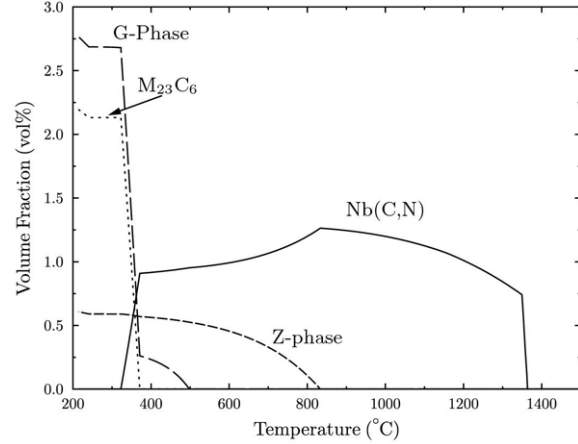


Fig. 3: Equilibrium phase fraction in mol % predicted by ThermoCalc using the TCFE6, and TTNI8 databases for the centrifugally cast 2032-Nb stainless steel chemistry in [Table 1](#).

Say some stuff about [Fig. 3](#). Now here is a figure with subfigures inside of it.

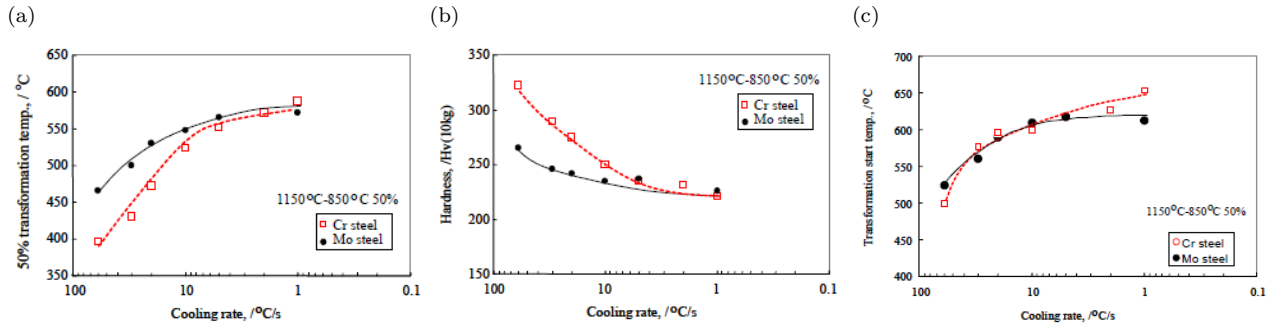


Fig. 4: Relationship between the change in cooling rate with the (a) 50% γ/α transformation temperature, (b) hardness, (c) γ/α start transformation temperature.

4. Discussion

4.1. Revised Objective Function

Since the actual value of the objective function is not important for this model, variables $y(p,i,j)$ and $z(p,i,j)$ can be optimized for each player by adding their cost products to the objective function.

$$\max z := \sum_{p \in P} \sum_{i \in N} \sum_{j \in M} c(i,j)x(p, i, j) \quad (6)$$

First of all, the resource matrix is converted into binary arrays for each of the five resources. for example:

$$lbr(i,j) = \begin{cases} 0, & \text{if } res(i,j) > 1 \\ 1, & \text{if } res(i,j) = 1 \end{cases}$$

For multiple equations

$$\sum_{i \in N} \sum_{j \in M} l(i,j)z(p,i,j) \leq 3(1 - \delta(p)) \quad \forall p \in \{1 \dots 4\}$$

$$\sum_{i \in N} \sum_{j \in M} b(i,j)z(p,i,j) \leq 3(1 - \delta(p)) \quad \forall p \in \{1 \dots 4\}$$

$$x(p,i,j) - w(i,j) \leq 3(\delta(9-p)) \quad \forall \{p \in \{4 \dots 8\}, i \in N, j \in M\}$$

5. Conclusions

Conclusions Section

6. Acknowledgement

This study has been supported by...

7. References

- [1] Mathes, B., Omladič, M., Radjavi, H.. Linear Spaces of Nilpotent Operators. *Linear Algebra Appl* 1991;149:215–225.
- [2] Knuth, D.E.. *The T_EXbook*. Addison-Wesley; 1984.
- [3] de Branges, L.. A construction of invariant subspaces. *Math Nachr* 1993;163:163–175.